

AN ABSTRACT OF THE THESIS OF

Barrett Henning Erickson for the Master of Science in Geophysics  
(Name) (Degree) (Major)

Date thesis is presented August 8, 1966

Title MARINE SEISMIC STUDIES NEAR NEWPORT, OREGON

*Redacted for Privacy*

Abstract approved \_\_\_\_\_  
(Major professor)

In July 1964 three seismic refraction profiles were recorded over Stonewall Bank (44° 32'N, 124° 24'W) to determine gross sub-bottom geological structure to depths of thousands of feet. In August 1964 a continuous seismic reflection profiler was used to document shallow geological structure within the rocks forming the Bank.

Stonewall Bank is composed of eastward dipping Pliocene siltstones which emerge westward from beneath unconsolidated Quaternary sediments. These siltstones form gentle dip slopes on the Bank's eastern flank but rougher topography is found on the top and western flank where the bedding planes intersect the sea floor at greater angles. Refraction data from this study indicate the siltstones thicken southward by 5000 feet over a six mile distance which accounts for almost all of the thickness change in the measured section. A deeper layer, 5000 feet thick, which appears to be Miocene may be exposed west of the Bank beneath the sediments. The base of this deeper layer has a southerly dip component of about six degrees and lies 12,000 feet below the southern end of the Bank.

Although this was the deepest interface encountered, the underlying material is not believed to be basement.

MARINE SEISMIC STUDIES  
NEAR NEWPORT, OREGON

by

BARRETT HENNING ERICKSON

A THESIS

submitted to

OREGON STATE UNIVERSITY

in partial fulfillment of  
the requirements for the  
degree of

MASTER OF SCIENCE

June 1967

APPROVED:

*Redacted for Privacy*

\_\_\_\_\_  
Professor of Oceanography  
In Charge of Major \_\_\_\_\_

*Redacted for Privacy*

\_\_\_\_\_  
Chairman of Department of Oceanography \_\_\_\_\_

*Redacted for Privacy*

\_\_\_\_\_  
Dean of Graduate School \_\_\_\_\_

Date thesis is presented August 8, 1966

Typed by Opal Grossnicklaus

## ACKNOWLEDGEMENTS

This research was conducted under the direction of Professor Joseph W. Berg, Jr., Department of Oceanography, Oregon State University. The author expresses his thanks and appreciation to Dr. Berg for his continuing help and guidance.

Valuable technical discussions were held with Professor Rod-erick Mesecar who supplied the design for the hydrophone preamplifier and with William Bales who designed and built the blasting box and associated components.

Many helpful discussions were held with Neil J. Maloney and James H. Whitcomb. Suryya Sarmah, John Livingston, Mark Odegard, Orin Knee, and Lynn Trembly helped obtain the data at sea.

This research was supported by the Office of Naval Research under Contract Nonr 1286(10), Project NRO 83-102, and was accomplished while the author was participating in the U. S. Navy Advanced Study Program sponsored by the Pacific Missile Range.

## TABLE OF CONTENTS

|   |    |
|---|----|
| I. INTRODUCTION .....                               | 1  |
| II. INSTRUMENTATION .....                           | 5  |
| Refraction Instrumentation .....                    | 5  |
| Reflection Instrumentation .....                    | 11 |
| III. EXPERIMENTAL PROCEDURES .....                  | 12 |
| Refraction Field Procedures .....                   | 12 |
| Reflection Field Procedures .....                   | 15 |
| IV. ANALYSIS OF DATA .....                          | 17 |
| Refraction Data .....                               | 17 |
| Topographic Corrections .....                       | 18 |
| Reference Surface Corrections .....                 | 19 |
| Calculation of Acoustic Velocity in Water .....     | 20 |
| Depth Determination .....                           | 27 |
| Reflection Data .....                               | 29 |
| V. DISCUSSION OF RESULTS .....                      | 32 |
| Surface Morphology .....                            | 32 |
| Layer A - Unconsolidated Quaternary Sediments ..... | 33 |
| Layer B - Pliocene Siltstones .....                 | 34 |
| Layer C .....                                       | 35 |
| Layer D .....                                       | 36 |
| VI. CONCLUSIONS .....                               | 38 |
| BIBLIOGRAPHY .....                                  | 39 |

## LIST OF FIGURES

| <u>Figure</u> |   | <u>Page</u> |
|---------------|---|-------------|
| 1.            | Index map and regional bathymetry                                     | 2           |
| 2.            | Block diagram of seismic refraction system                            | 6           |
| 3.            | Typical response curves of amplifier-filter system                    | 9           |
| 4.            | Index map of refraction and reflection survey lines                   | 13          |
| 5.            | Travel time curves - profile 1  | 24          |
| 6.            | Travel time curves - profile 2  | 25          |
| 7.            | Travel time curves - profile 3  | 26          |
| 8.            | Idealized structural section from refraction survey<br>(see Figure 4) | 28          |
| 9.            | Structure determined from reflection survey                           | 31          |

## LIST OF TABLES

| <u>Table</u> |                             | <u>Page</u> |
|--------------|-----------------------------|-------------|
| 1.           | Refraction data - profile 1 | 21          |
| 2.           | Refraction data - profile 2 | 22          |
| 3.           | Refraction data - profile 3 | 23          |

# MARINE SEISMIC STUDIES NEAR NEWPORT, OREGON

## INTRODUCTION

The purpose of this research was to conduct a seismic refraction survey in the vicinity of Stonewall Bank, off Newport, Oregon, and make a geological interpretation of the data. As shown in Figure 1, Stonewall Bank is an anomalous feature on the central continental shelf about 14 miles west of the Oregon coast line. Depths of less than 20 fathoms occur in the southern portion which is divided in two parts by a conspicuous eastward trending valley. The 40-fathom contour outlines an area 12 miles long by four miles wide trending just west of north. The Bank is considered to be located on the west flank of a structural basin lying to the east and north; the east flank is evident as westward dipping tertiary beds on the coast. Maloney and Byrne (2) describe all rock samples collected in the vicinity of the Bank as varieties of siltstone. The southern part of the Bank has been dated as Pliocene from biostratigraphic analyses of four samples; the northern part has been tentatively dated as at least partly Miocene from analysis of one sample. Remaining samples collected by the Oregon State University, Department of Oceanography, on the north Bank have been barren of fossils (Neil J. Maloney, personal communication).

The continental shelf has been the site of rather intensive



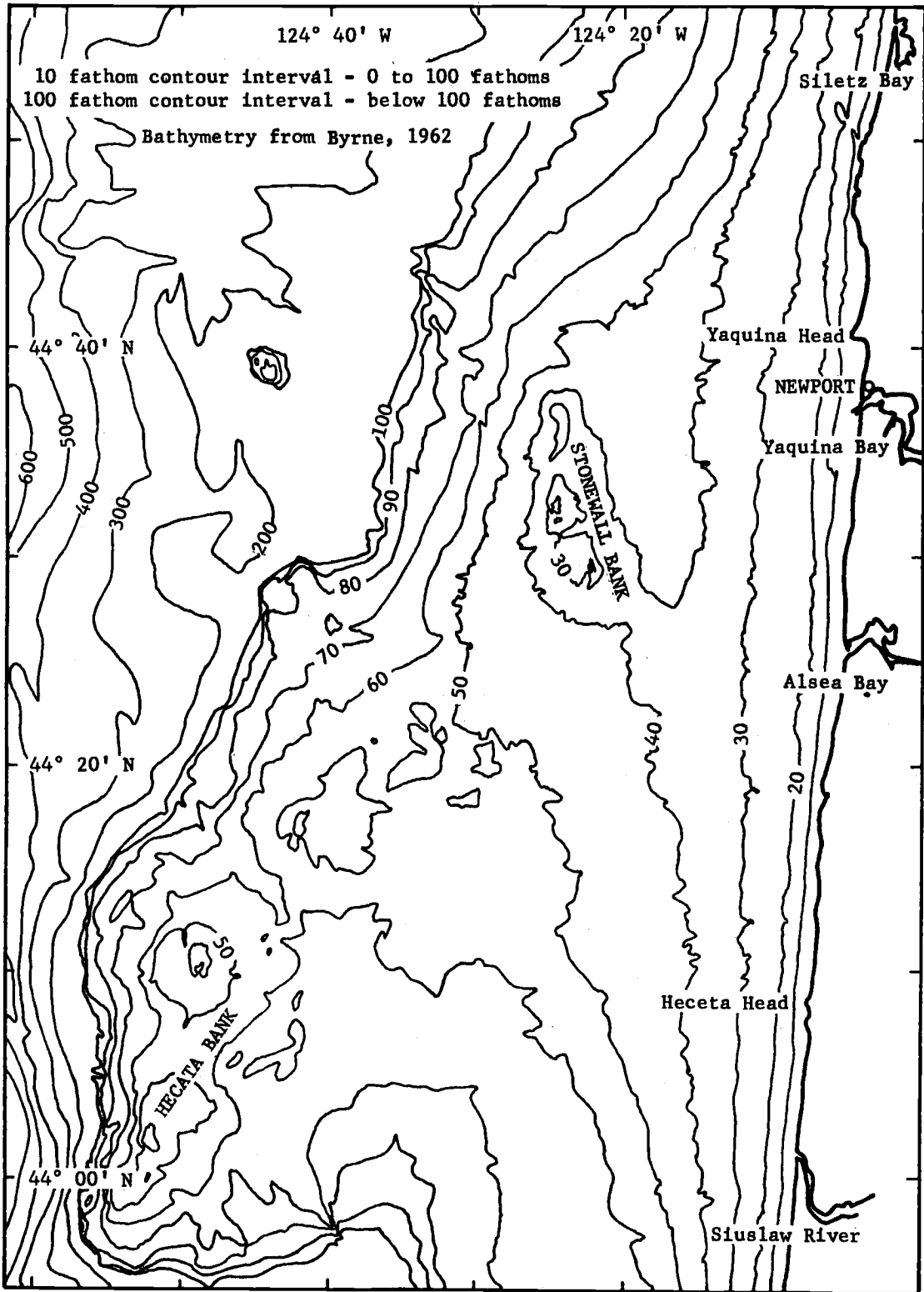


Figure 1. Index map and regional bathymetry

investigations by many major oil companies. The results of these investigations have not been available to the public for economic reasons and little is known of the structure or stratigraphy from these sources. Scripps Institution of Oceanography has conducted magnetic surveys off the West Coast of the United States, including Oregon in past years. These data have been complemented by additional magnetic and gravity surveys made by the Geophysics Research Group of Oregon State University during 1963 and 1964.

Gravity and magnetic data from this region have been analyzed by Whitcomb (5) who concluded that the axis of a north-south structural syncline lies between Stonewall Bank and the coast line with basement depths of about 20,000 feet. Gravity interpretation indicated this axis may shift westward with depth. In the vicinity of the Bank continuous reflection profiles analyzed by Whitcomb showed a generally east dipping structure with complex minor folding and faulting which is covered eastward from the Bank by recent unconsolidated sediments.

In view of the limited knowledge of the structure of the continental shelf in this region, it was considered that a seismic refraction study in the vicinity of Stonewall Bank would complement previous gravity, magnetic, and geological studies. A study was initiated which consisted of designing a seismic refraction instrumentation system around available amplifiers and a recorder, shooting refraction

profiles over Stonewall Bank, analyzing the refraction data, and drawing conclusions regarding possible geologic structure in the vicinity of the Bank. A seismic reflection profiler was used to study anomalous portions of the refraction profiles that were attributed to shallow geologic structures.

## INSTRUMENTATION

Instrumentation for both refraction and continuous reflection measurements were used in this study. The instrumentation system for the refraction work was, for the most part, designed and built as part of this project. The continuous reflection profiles, however, were obtained with the use of commercially built equipment.

### Refraction Instrumentation

A marine seismic refraction survey normally requires two ships, one which carries receiving equipment and one from which explosives are detonated in the water at proper times and places. The instrumentation system on the receiving ship must receive and amplify the pressure waves which have traveled through the earth and water. After amplification the signals must be separated into various frequency bands and recorded along with an accurate time base. The shooting vessel must carry instrumentation to detonate the explosives and transmit the time of the explosion to the receiving ship. This usually requires a radio link between the two ships. The block diagram of the system used for this study is shown in Figure 2. Each of the components will be discussed in order.

Two REMACO Model R-100 hydrophones were obtained. These consisted of an encapsulated barium titanate crystal attached to a

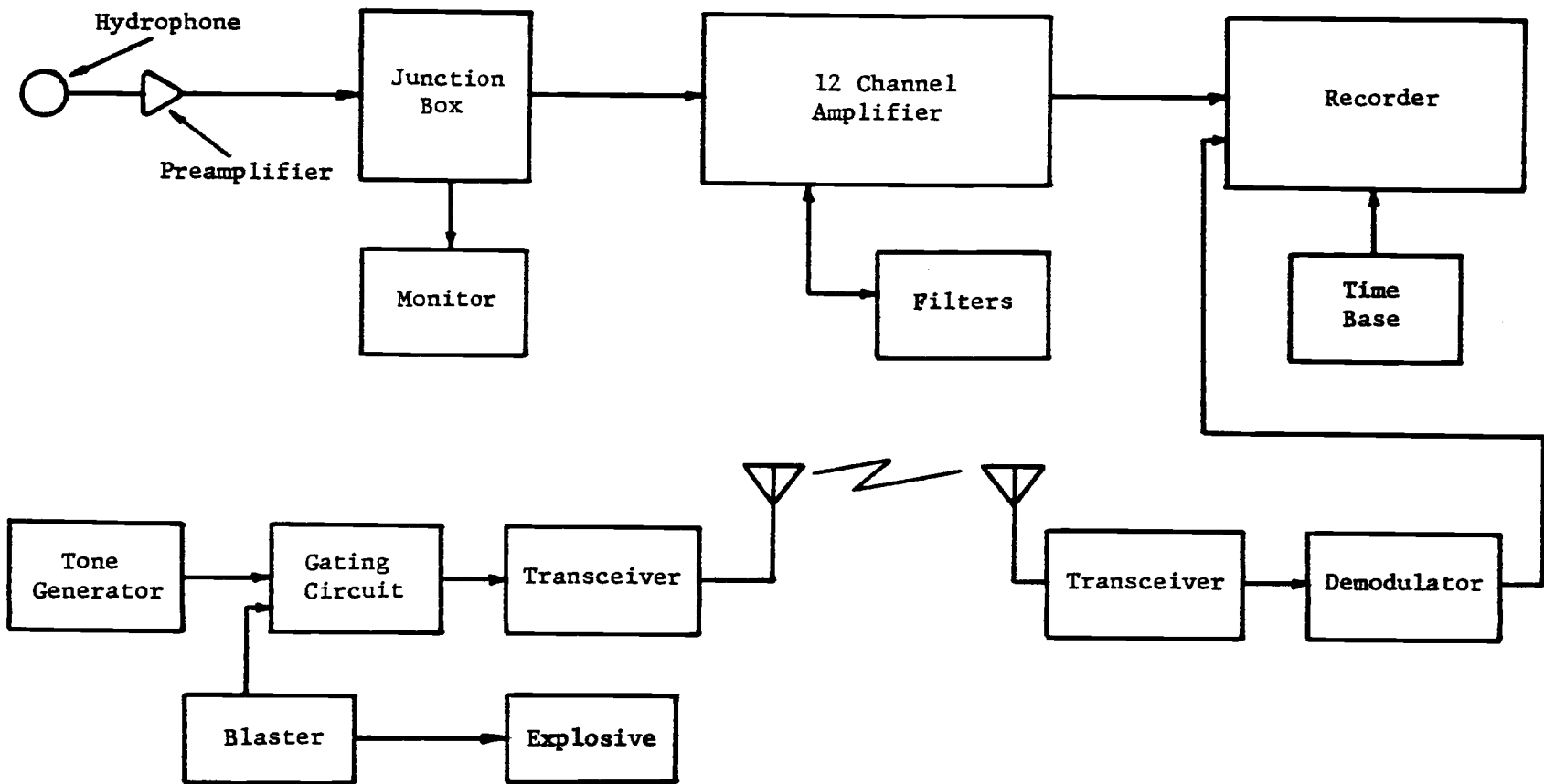


Figure 2. Block Diagram of Seismic Refraction System

stainless steel case with a 2" x 10" preamplifier cavity. The crystals had a sensitivity of approximately -80 dbv per microbar for the frequency range two cps to 20 kcs. A solid state preamplifier was built, tested, and installed in each of the hydrophones. The gain characteristics of the preamplifier, Figure 3, show that the response was flat within  $\pm 3$  db from 5 to 1,000 cps. Each hydrophone was attached to 500 feet of Belden, No. 8407, shielded, heavy duty power cable which contained four #16 stranded copper conductors. This cable provided both the strength and flexibility needed for handling aboard ship. Two conductors were used as signal leads with the other two available for future use as power leads or for insertion of a calibration signal.

The shipboard end of the cable was connected to a junction box which provided test points from which to monitor the hydrophone outputs (see Figure 2). The junction box also allowed the inputs of all amplifiers to be placed in parallel and connected to either of the hydrophones or to an external input for test purposes. A Hewlett-Packard AC transistorized volt meter, Model 403A, was used to monitor the hydrophone output. Ambient noise levels could, therefore, be measured and malfunctions detected.

The refraction amplifiers and recorder were the nucleus of the system. The amplifiers were part of a Mid-Western Instruments Model 475 12-channel portable refraction unit originally designed for

use with 12 geophones. The gain of each channel was independently variable from 0 to 78 db. The original frequency response of each channel is shown by curve "A" in Figure 3. For this study the system was required to handle outputs of two hydrophones in each of the three frequency bands: 5-100 cps, above 300 cps, and broadband (see Figure 3). The output of each hydrophone was connected to four separate amplifier channels. Two of these channels were used with staggered gains to increase the dynamic range for broadband recording. The other two channels were used as preamplifiers for the high and low pass filters. Only two stages of these preamplifier channels were used, the second stage acting as a cathode follower to match the 600 ohm input impedance of the Allison Model 2A filters. These were passive LC filters with greater than 30 db per octave attenuation above or below the cut off frequency which was adjustable between 15 cps and 10 kc. The filter outputs were connected directly to the remaining four amplifier channels. The frequency response of the band pass and high pass channels was modified as shown by curve "B" in Figure 3 to increase the response above 25 cps. Typical response curves of the amplifiers with the filters in the circuit are shown by curves "C" and "D" in Figure 3.

A Midwestern Instruments Model 534 14-channel oscillographic camera was used with Midwestern Instruments MI-EA (serial no.) F3.5 110-200 galvanometers. The galvanometers were driven by

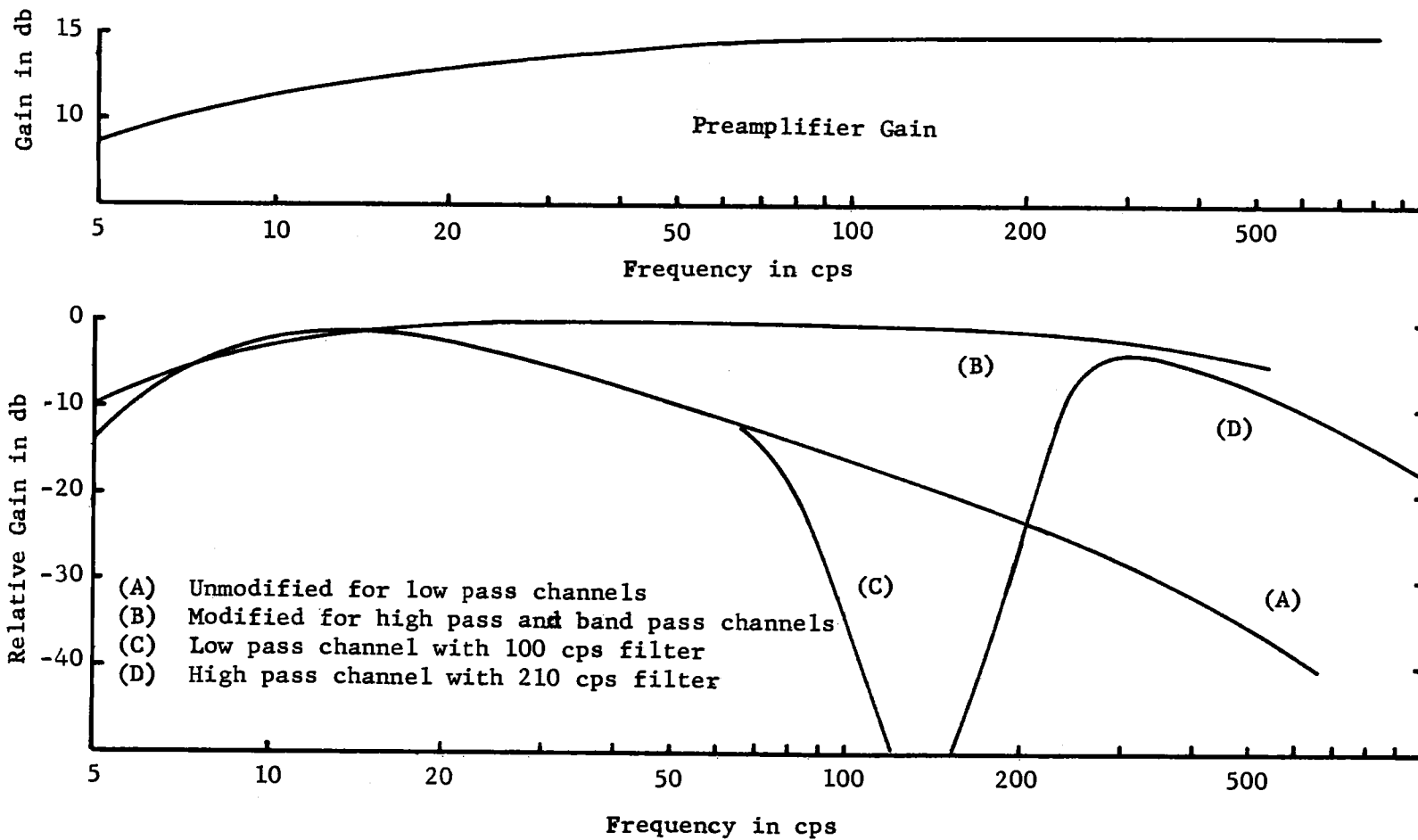


Figure 3. Typical Response Curves of Amplifier - Filter System



the amplifiers and the traces recorded on Kodak Linograph No. 480, specification one, photographic recording paper driven at 12 inches per second. The response of the galvanometers decreased for frequencies above 50 cps at approximately 4 db per octave. This was not considered significant as the predominant seismic energy is below 50 cps. Ample gain was available in the amplifiers and no problem was encountered in receiving the higher frequency energy traveling through the water. Integral with the recorder was a time base generator comprised of a 100 cps tuning fork precision frequency power supply which drove a synchronous motor. The motor rotated a barrel with ten longitudinal slits at ten revolutions per second. These slits gated a light beam which exposed lines of light on the recording paper at intervals of 0.01 seconds providing an accurate relative time base for determining the travel times of the seismic waves.

A blasting box was constructed to detonate electrically the explosive charges. Upon closing the firing circuit, the surge of current caused a gating circuit to remove a 1300 cps tone modulation from the carrier of the radio transmitter. The cessation of the tone thus coincided with the surge of current which detonated the explosives.

Two five-watt Heath Citizen band transceivers were used for communications between the ships and for transmitting the shot time

to the receiving ship. On the receiving ship the audio output of the transceiver was connected to a demodulator which passed the signal through a sharp 1300 cps band pass filter and rectified it. The output was connected to one of the galvanometers in the oscillographic recorder. The time of the explosion indicated by the cessation of the 1300 cps tone was, therefore, marked by a sharp deflection of the galvanometer trace on the record.

#### Reflection Instrumentation

Equipment for the seismic reflection studies was a modified Alpine Geophysical Associates, Inc. Model 440, Continuous Stratification Profiler which used a high energy spark discharge as a repetitive source. The spark source and three hydrophones, two of which were the type previously described, were towed astern of the ship while making the survey. Signals from the three hydrophones were mixed, passed through appropriate filters, and recorded. This equipment has been described in greater detail by Whitcomb (5, p. 7-10).

## EXPERIMENTAL PROCEDURES

The data for this study were acquired during survey cruises in July and August 1964. Four refraction profiles, two of which were to be reversals of each other, were planned to be shot over Stonewall Bank using the instrumentation previously described. Operational circumstances, however, allowed only three profiles to be shot, none of which could be considered reversed in the strict meaning of the word (See Figure 4a). From an analysis of the results of these refraction profiles, further examination of a portion of Stonewall Bank with the Seismic reflection profiler seemed warranted.

### Refraction Field Procedures

On 6, 7, 8, and 9 July 1964 three seismic refraction profiles were recorded over Stonewall Bank at the locations shown in Figure 4a. Two ships were used, the RV ACONA operated by the Department of Oceanography of Oregon State University and the MV TELESIS, a chartered vessel. The ACONA, used as the receiving ship, carried four scientific personnel plus the receiving and recording equipment. The TELESIS, used as the shooting ship, carried three scientific personnel plus explosives and blasting equipment. The ACONA took station and anchored using a Danforth anchor on the end of the main hydrographic wire. Two hydrophones were lowered to

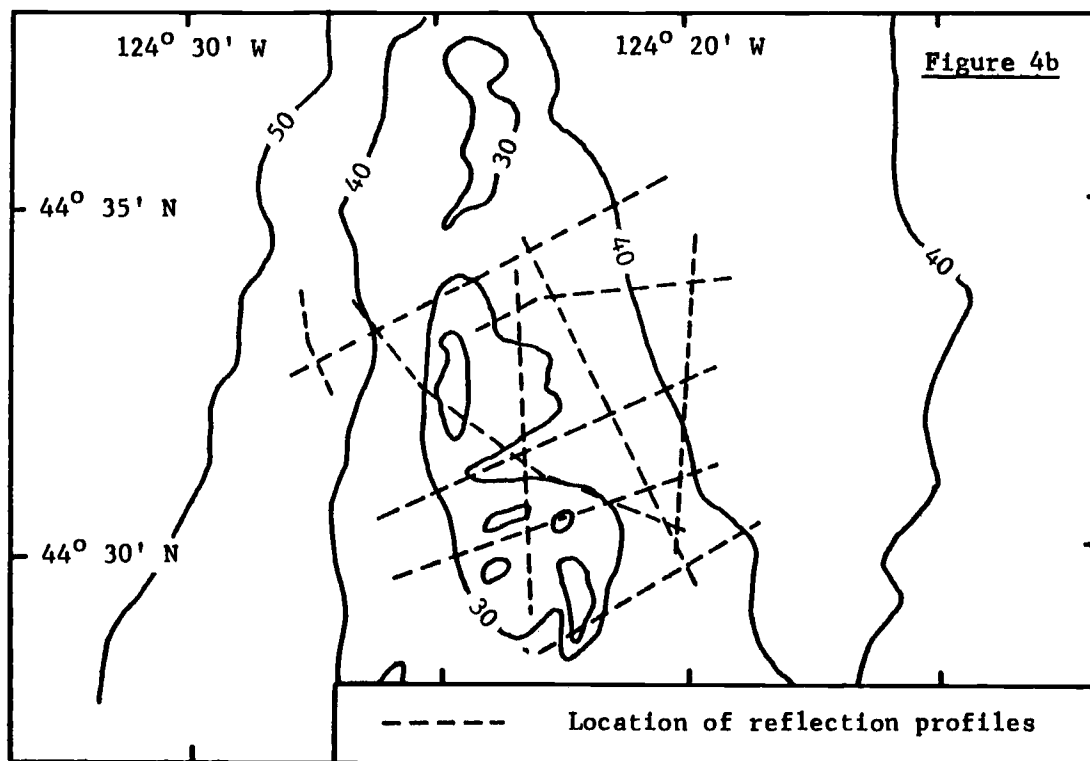
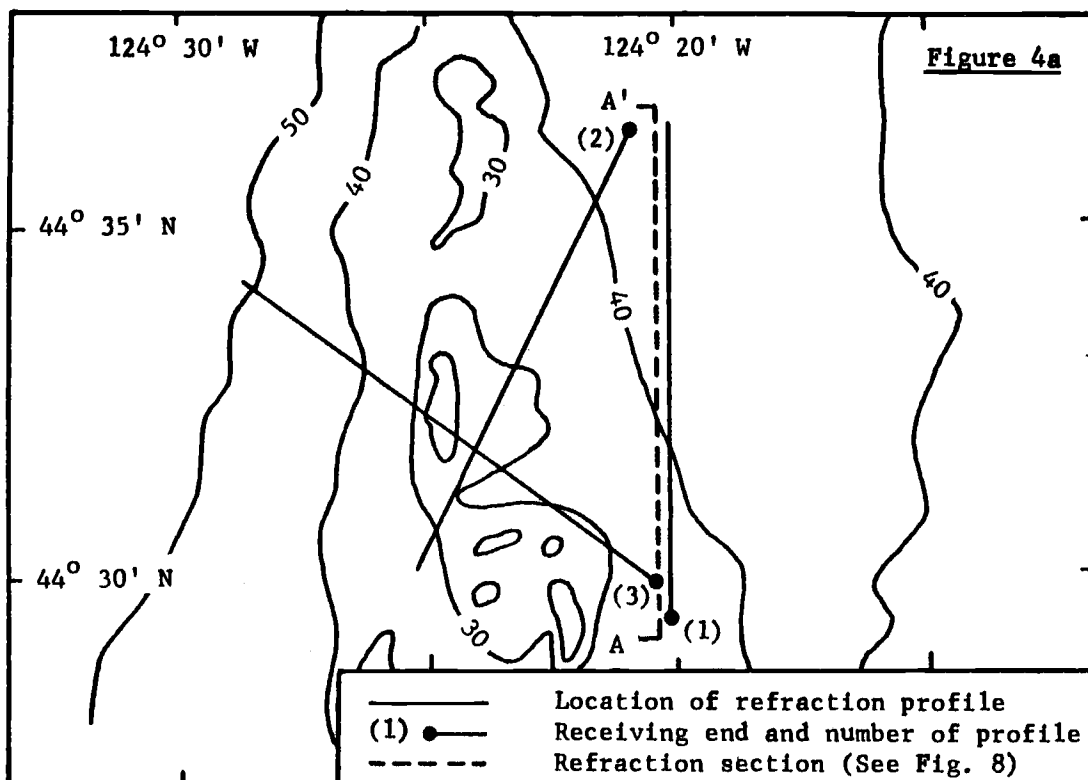


Figure 4. Index map of refraction and reflection survey lines

the bottom from opposite ends of the starboard rail. Between shots the hydrophones were raised off the bottom.

The TELESIS detonated explosive charges ranging from one to 40 pounds, with DuPont SSS EB caps fired through 1,000 feet of #16 POT wire. Each charge, up to five pounds, was comprised of one Nitramon "S" booster and one or more one pound charges of Nitramon. Each charge larger than five pounds was comprised of a water work booster and combinations of Nitramon WW ten and 20 pound charges. After each shot the TELESIS circled back to ascertain if any fish had been killed by the explosion. To minimize the fish kill, echo sounder records were examined before each shot to determine if any schools of fish were present.

During the one-minute countdown on the radio prior to each shot, personnel on the receiving vessel lowered the hydrophones to the bottom, checked the instrumentation, and prepared to record. At ten seconds prior to shot time personnel on the shooting vessel placed the 1300 cps tone on the radio and at one second prior to shot time the recorder was started. After the water wave was received the recorder was stopped, the paper developed and inspected, and the travel times of the pressure pulses were read. The travel times were then plotted to insure that acceptable records were being received and large enough charges were being used to get reception of the first ground arrivals.

Position of the ACONA at anchor was determined by radar fixes and horizontal sextant angles from the coastal land marks. The anchor was lost sometime during the survey on the 8th of July, but this was not discovered until the shooting had been completed. Poor holding ground was encountered on the 9th of July and the ship dragged anchor to the south for about one mile.

The TELESIS used its radar to take shooting stations locations from the ACONA out to distances of about five miles. Beyond this distance the radar on the TELESIS could not detect the ACONA and the remainder of the stations were occupied by dead reckoning. However, water wave travel times gave distances between the TELESIS and the ACONA for all shots.

A bathythermograph was lowered to the bottom from the ACONA twice a day. This provided temperature information, from which the velocity of sound in the water could later be computed using suitable salinity values.

#### Reflection Field Procedures

On 18 and 19 August a grid of continuous seismic reflection profiles were made using the R/V ACONA. Independent bathymetric measurements were made concurrently with an AN/UQN-1 echo sounder and Precision Depth Recorder. The spark sound source was trailed immediately aft from the fantail while the three

hydrophones were independently trailed from a boom off the starboard beam. During the 18-hour cruise the ACONA averaged about four knots. Positions were determined by the ship's crew every 15 minutes from LORAN readings and radar ranges and bearings from selected landmarks. These positions were recorded and plotted on C&GS Chart No. 6056 and are shown in Figure 4b. Inadequate navigation records precluded the use of some reflection data.

The continuous reflection data was subjected to half-wave rectification and recorded in two frequency ranges, 90 to 300 cps and 300 to 900 cps. The records displayed information which was received between zero and one-half second after each spark, i. e., full scale represented depths from the surface to about 1200 feet.

## ANALYSIS OF DATA

Upon completion of the surveys, the records were carefully analyzed in order that meaningful conclusions might be drawn from the data. The refraction records were reviewed several times in order to identify all valid arrivals. Corrections were made to refer all data to the same reference surface. The reflection records were also reviewed several times to insure that the reflections were real and consistent, and the interpretation was reasonable.

### Refraction Data

The 71 seismic records obtained along the three profiles were carefully examined and the arrival times of the water wave and first ground wave energy identified and marked. Travel times were then determined by measuring the time interval between the shot break and the arrival of each seismic wave. Tentative plots of ground wave travel time vs. water wave travel time were made and straight lines fitted to these points by eye. The records were then re-examined for possible missing first arrivals and for any discernible later arrivals which would correlate with those already plotted. At ranges less than about five miles the first arrivals were generally very apparent but beyond this range they were often emissive and frequently difficult to distinguish from the background noise. After



all arrival times were picked and checked, straight lines were fitted to all the points identified with each travel path using least squares and the slopes and intercept times of the lines were used for subsequent analysis. It should be noted, however, that the arrivals which traveled via the deepest interface encountered were weak and few in number especially on profile 1. Water wave arrivals reflected one or more times from the surface and floor of the shallow sea dominated the records for periods of several seconds after the direct water wave arrival and hence obscured any refracted waves arriving during that period.

#### Topographic Corrections

The maximum bottom topographic changes encountered along the refraction profiles were approximately 20 fathoms. The topographic correction was computed by the following relation from Officer (4, p. 29)

$$t_t = \frac{\Delta d_t}{c_o} \cos(\sin^{-1} c_o / c_{na}) - \frac{\Delta d_t}{c_x} \cos(\sin^{-1} c_x / c_{na}) \quad (1)$$

where  $t_t$  is the topographic correction in seconds,  $\Delta d_t$  is the topographic change in feet,  $c_o$  is the velocity of sound in sea water in feet per second, and  $c_x$  is the velocity of sound in the material which is responsible for the topographic change in feet per second.

For a water velocity of 4850 feet per second, bottom velocity of 6200 feet per second, and an apparent velocity for the ground arrival of 8000 feet per second the topographic correction for 20 fathoms is less than 0.01 seconds. This was considered to be negligible in view of the difficulty in picking the beginnings of emissive arrivals with confidence to better than a few hundredths of a second. Consequently, no topographic corrections were made to the data.

#### Reference Surface Corrections

The hydrophones were located on the ocean bottom in approximately 200 feet of water while the explosives were nominally detonated at 50 feet below the water surface. Corrections were, therefore, made to the observed travel times so that they would correspond to the times which would have been observed if both hydrophones and explosives were at sea level. This correction was computed by the following relation from Officer (4, p. 28)

$$t_{sr} = \frac{\Delta d_s}{c_o} \cos(\sin^{-1} c_o/c_{na}) + \frac{\Delta d_h}{c_o} \cos(\sin^{-1} c_o/c_{nb}) \quad (2)$$

where  $\Delta d_s$  and  $\Delta d_h$  are the depths in feet of the shot and hydrophone respectively,  $c_o$  is the velocity of sound in water in feet per second,  $c_{na}$  and  $c_{nb}$  are the apparent velocities of the ground arrivals measured at the receiving and shooting ends of the reversed profile

respectively. Because of the small depths involved and the lack of a true reversed profile, the same apparent velocity,  $c_{na}$ , was used in both terms. When  $d_s$  and  $d_h$  are considered to be constant as was done in this work, the only variable is  $c_{na}$  and the correction results in a change of intercept time and not of slope. For this work, the datum corrections ranged from 0.02 to 0.06 seconds.

#### Calculation of Acoustic Velocity in Water

Vertical acoustic velocity profiles were computed from the bathythermograph observations assuming a salinity of 33‰ using the following relation:

$$c = 141,000 + 110S + 0.018d + (421t - 3.7t^2) \quad (3)$$

where  $c$  is the velocity of sound in cm/sec,  $S$  is the salinity in parts per thousand,  $d$  is the depth in cm, and  $t$  is the temperature in degrees Celsius. From these profiles an average vertical velocity of 1.48 km/sec (4850 feet per second) was selected for use in subsequent calculations.

The water wave travel time, the ground wave travel time, and the corrected ground wave travel time are listed for each shot in Tables 1, 2, and 3. Travel time curves, together with the intercept times are shown in Figures 5, 6, and 7.

Table 1. Refraction Data - Profile 1

| Layer          | Shot No.       | Water Wave* | Ground Wave* | Corrected Ground Wave* |
|----------------|----------------|-------------|--------------|------------------------|
| A              | 2              | 0.318       | 0.286        | 0.308                  |
|                | 3              | 0.503       | 0.451        | 0.473                  |
|                | 4              | 0.948       | 0.845        | 0.867                  |
|                | 5              | 0.971       | 0.863        | 0.885                  |
|                | 6              | 1.252       | 1.104        | 1.126                  |
|                | 7              | 1.654       | 1.477        | 1.499                  |
|                | 8              | 1.983       | 1.761        | 1.783                  |
|                | B <sub>a</sub> | 4           | 0.948        | 0.786                  |
| 5              |                | 0.971       | 0.804        | 0.836                  |
| 6              |                | 1.252       | 1.021        | 1.053                  |
| 7              |                | 1.654       | 1.325        | 1.357                  |
| 8              |                | 1.983       | 1.581        | 1.613                  |
| 14             |                | 5.349       | 4.179        | 4.211                  |
| 15             |                | 6.590       | 6.156        | 5.188                  |
| 17             |                | 7.216       | 5.65         | 5.68                   |
| 18             |                | 7.818       | 6.142        | 6.174                  |
| 19             |                | 8.178       | 6.41         | 6.44                   |
| 20             |                | 8.300       | 6.555        | 6.587                  |
| 21             |                | 8.425       | 6.642        | 6.674                  |
| 22             |                | 8.682       | 6.85         | 6.88                   |
| 23             |                | 8.964       | 7.06         | 7.09                   |
| 24             | 9.132          | 7.19        | 7.22         |                        |
| B <sub>b</sub> | 9              | 2.282       | 1.801        | 1.835                  |
|                | 10             | 2.630       | 2.059        | 2.093                  |
|                | 11             | 3.021       | 2.351        | 2.385                  |
|                | 12             | 3.510       | 2.702        | 2.736                  |
|                | 13             | 4.394       | 3.348        | 3.382                  |
| C              | 18             | 7.718       | 6.065        | 6.108                  |
|                | 20             | 8.300       | 6.325        | 6.368                  |
|                | 22             | 8.682       | 6.49         | 6.533                  |
|                | 23             | 8.964       | 6.66         | 6.70                   |
| D              | 19             | 8.178       | 6.133        | 6.179                  |
|                | 21             | 8.425       | 6.232        | 6.278                  |

\* Travel time in seconds.

Table 2. Refraction Data - Profile 2

| Layer | Shot No. | Water Wave* | Ground Wave* | Corrected Ground Wave* |
|-------|----------|-------------|--------------|------------------------|
| A     | 1        | 0.254       | 0.233        | 0.259                  |
|       | 2        | 0.454       | 0.483        | 0.509                  |
|       | 3        | 0.646       | 0.585        | 0.611                  |
|       | 5        | 1.136       | 1.025        | 1.051                  |
|       | 6        | 1.419       | 1.277        | 1.303                  |
|       | 7        | 1.536       | 1.366        | 1.392                  |
|       | B        | 5           | 1.136        | 0.958                  |
| 6     |          | 1.419       | 1.193        | 1.233                  |
| 7     |          | 1.536       | 1.284        | 1.324                  |
| 2     |          | 2.285       | 1.839        | 1.879                  |
| 3     |          | 3.504       | 2.751        | 2.791                  |
| 4     |          | 3.961       | 3.133        | 3.173                  |
| 5     |          | 4.219       | 3.29         | 3.33                   |
| 6     |          | 4.496       | 3.52         | 3.56                   |
| C     | 3        | 3.504       | 2.68         | 2.73                   |
|       | 4        | 3.961       | 3.033        | 3.083                  |
|       | 5        | 4.219       | 3.189        | 3.239                  |
|       | 6        | 4.496       | 3.33         | 3.38                   |
|       | 8        | 4.707       | 3.494        | 3.544                  |
|       | 9        | 5.055       | 3.763        | 3.786                  |
|       | 12       | 5.400       | 3.909        | 3.959                  |
|       | 13       | 5.809       | 4.15         | 4.20                   |
|       | 14       | 6.414       | 4.551        | 4.601                  |
|       | D        | 9           | 5.055        | 3.736                  |
| 11    |          | 5.494       | 3.888        | 3.948                  |
| 12    |          | 5.400       | 3.82         | 3.88                   |
| 13    |          | 5.809       | 3.9          | 3.96                   |
| 15    |          | 6.757       | 4.36         | 4.42                   |

\* Travel time in seconds.

Table 3. Refraction Data - Profile 3

| Layer          | Shot No.       | Water Wave* | Ground Wave* | Corrected Ground Wave* |
|----------------|----------------|-------------|--------------|------------------------|
| B <sub>a</sub> | 2              | 0.175       | 0.152        | 0.177                  |
|                | 3              | 0.323       | 0.263        | 0.288                  |
|                | 4              | 0.487       | 0.418        | 0.443                  |
|                | 5              | 0.776       | 0.667        | 0.692                  |
|                | 6              | 1.174       | 0.993        | 1.018                  |
|                | 7              | 1.805       | 1.501        | 1.526                  |
|                | 8              | 2.479       | 2.065        | 2.090                  |
|                | 9              | 3.184       | 2.634        | 2.659                  |
|                | 10             | 3.816       | 3.133        | 3.158                  |
|                | 13             | 6.248       | 5.142        | 5.167                  |
|                | 14             | 6.719       | 5.471        | 5.496                  |
|                | 16             | 7.312       | 5.955        | 5.980                  |
|                | B <sub>b</sub> | 4           | 0.487        | 0.433                  |
| 5              |                | 0.776       | 0.667        | 0.695                  |
| 6              |                | 1.174       | 0.957        | 0.985                  |
| 7              |                | 1.805       | 1.442        | 1.470                  |
| 9              |                | 3.184       | 2.444        | 2.472                  |
| C              | 13             | 6.248       | 5.002        | 5.037                  |
|                | 14             | 6.719       | 5.301        | 5.336                  |
|                | 16             | 7.312       | 5.605        | 5.640                  |
|                | 19             | 8.680       | 6.35         | 6.38                   |
|                | 20             | 9.20        | 6.65         | 6.68                   |
|                | 23             | 10.161      | 7.254        | 7.289                  |
| D              | 13             | 6.248       | 5.002        | 5.042                  |
|                | 14             | 6.719       | 5.201        | 5.241                  |
|                | 16             | 7.312       | 5.39         | 5.43                   |
|                | 20             | 9.20        | 6.26         | 6.30                   |
|                | 22             | 10.405      | 6.43         | 6.47                   |
|                | 23             | 10.161      | 6.424        | 6.464                  |

\* Travel time in seconds.

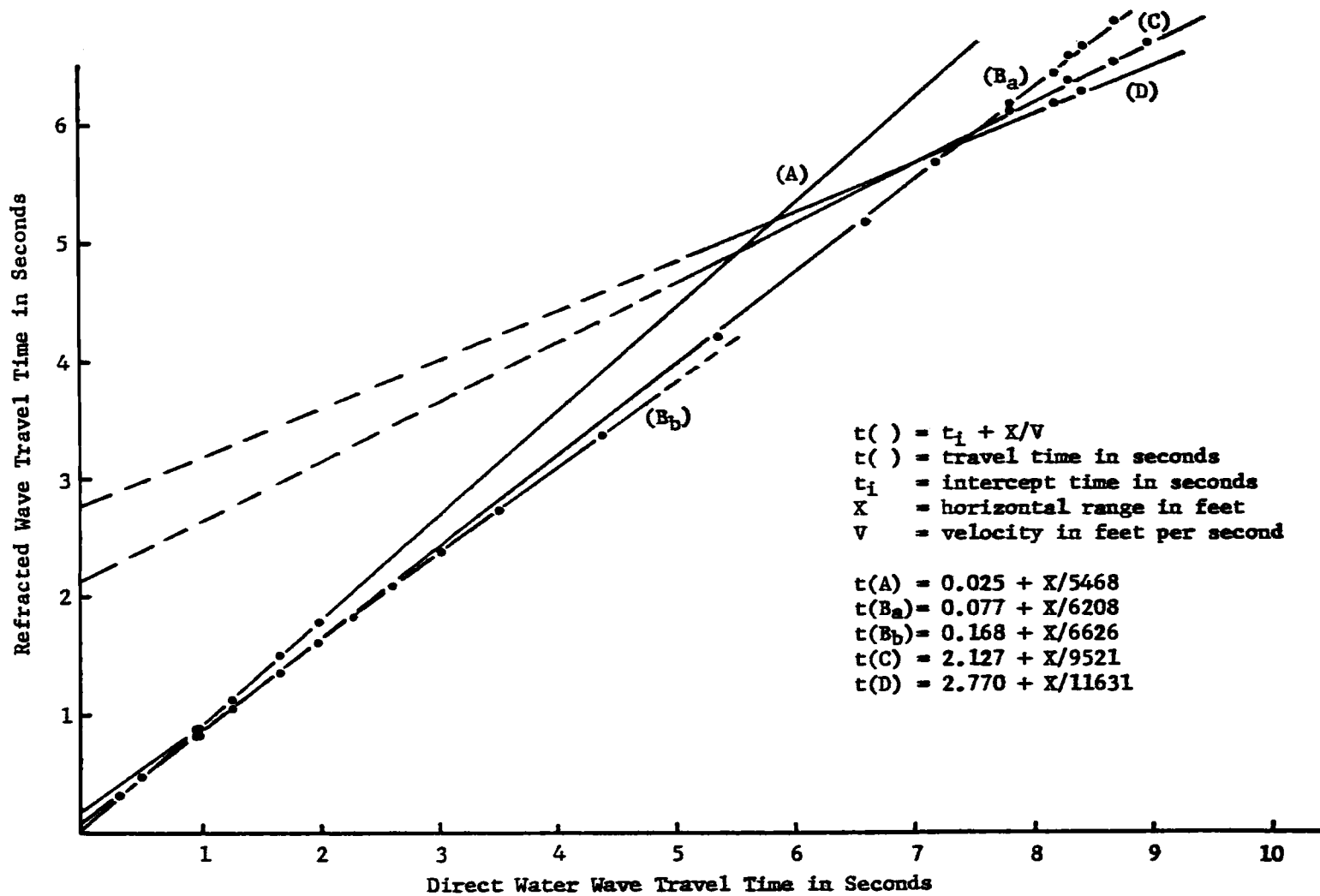


Figure 5. Travel Time Curves - Profile 1.

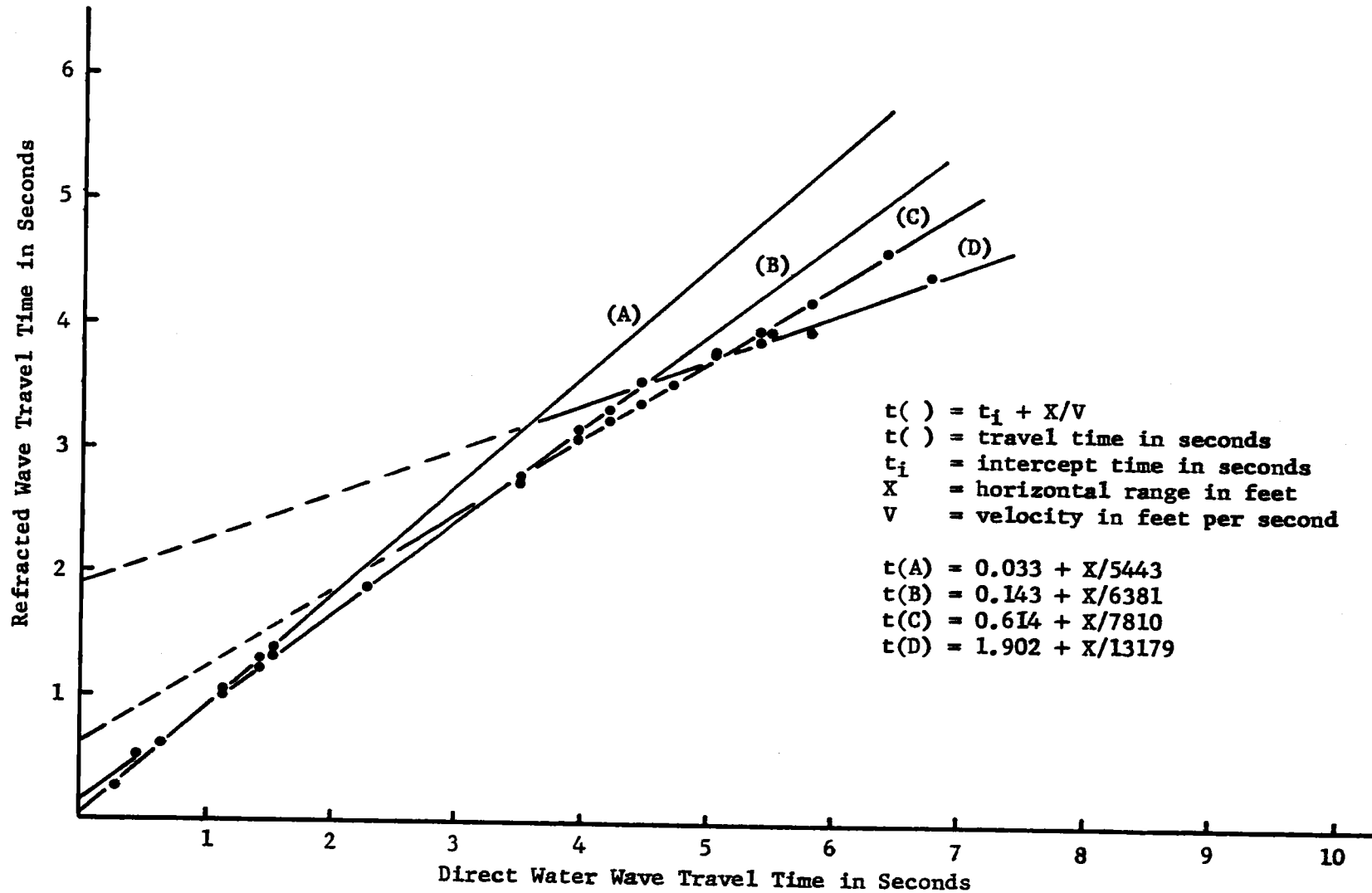


Figure 6. Travel Time Curves - Profile 2.



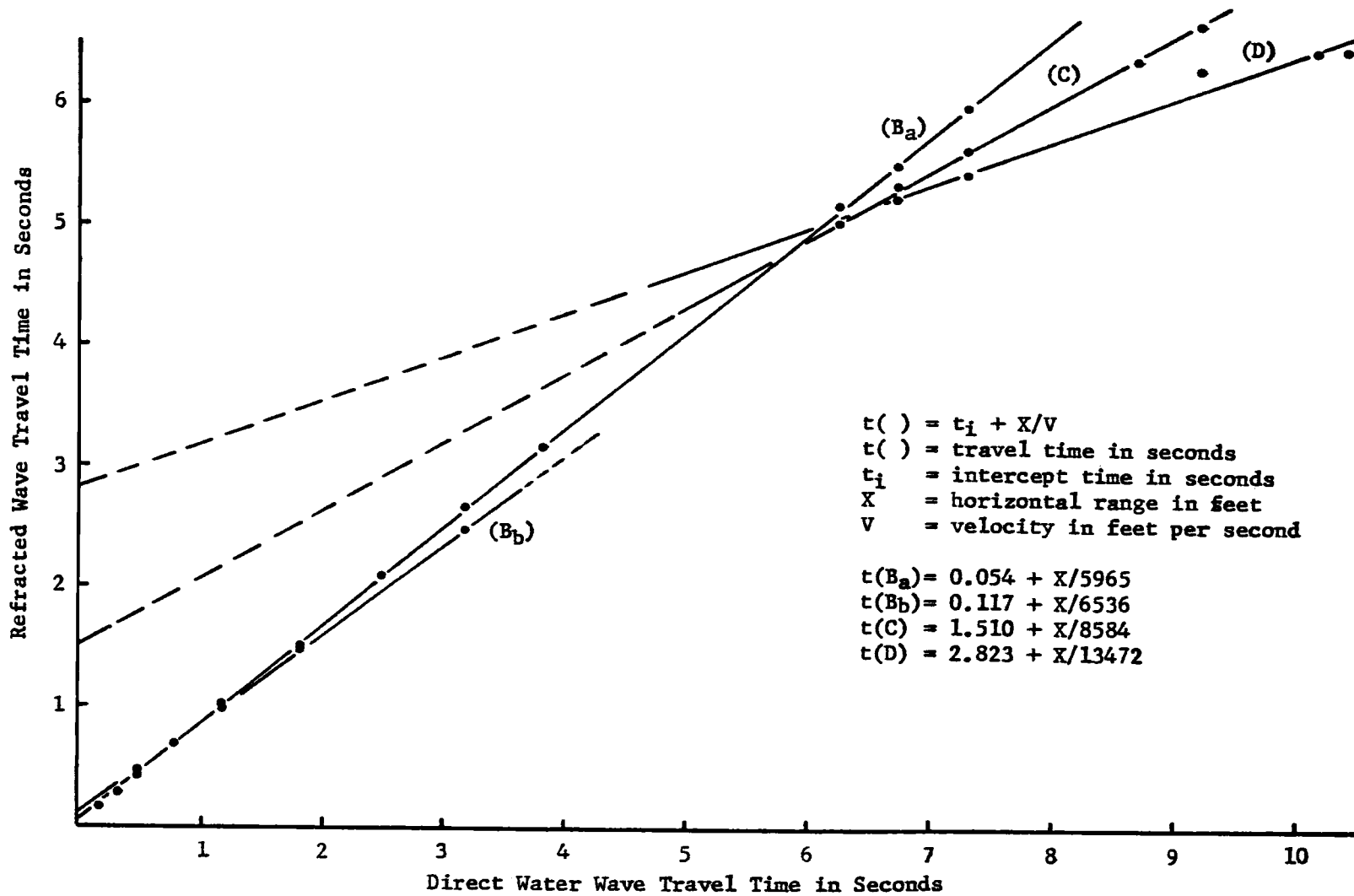


Figure 7. Travel Time Curves - Profile 3.

### Depth Determination

True velocities, dips, and depths may be calculated from the intercept times and apparent velocities of reversed refraction profiles. Procedures for this are described by Officer (3, p. 243-248). When profiles have not been truly reversed, which is the case in this study, then assumptions must be made regarding the true velocity before calculations are made. Horizontal beds characterized by constant velocities were assumed for the purpose of analysis. Depth computations were made using equations given by Officer (3, p. 239-242) as follows:

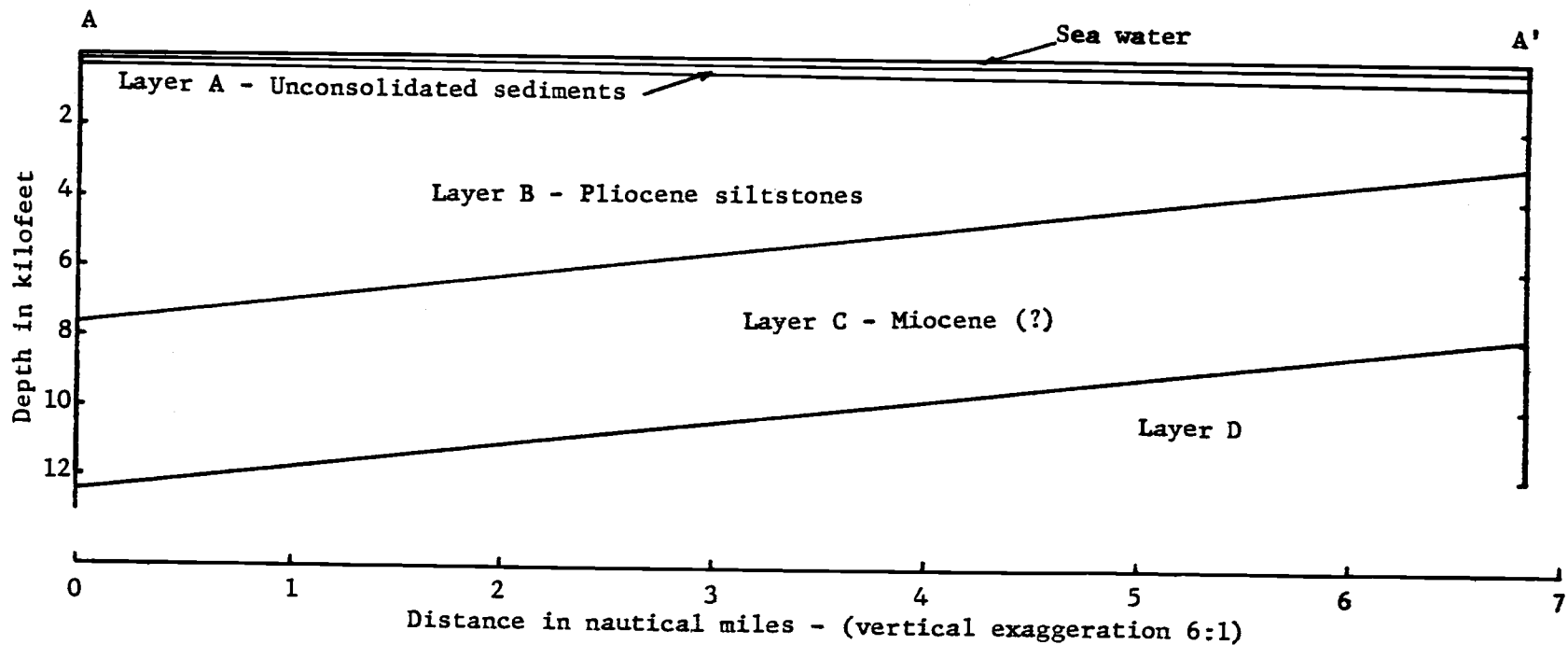
$$t_m = 2 \sum_{n=0}^{m-1} \frac{h_n}{c_n} \cos a_{nm}$$

$$a_{nm} = \sin^{-1} \frac{c_n}{c_m}; n = 0, 1, 2, \dots, m-1 \quad (4)$$

where,

$t_m$  is the intercept time for the  $m^{\text{th}}$  layer,  $h_n$  is the thickness of the  $n^{\text{th}}$  layer, and  $c$  is the true acoustic velocity.

Results of the depth calculations shown in Figure 8 were based on the velocity and intercept times shown in Figures 5, 6, and 7.



| Profile | Velocities, ft/sec. |       |       |        | Thickness, ft. |      |       | Depth to top, ft. |     |       |       |
|---------|---------------------|-------|-------|--------|----------------|------|-------|-------------------|-----|-------|-------|
|         | A                   | B     | C     | D      | A              | B    | C     | A                 | B   | C     | D     |
| 1       | 5468                | 6417* | 9521# | 11631# | 249            | 9160 | 2876# | 131               | 380 | 9540# | 12416 |
| 2       | 5443                | 6381  | 7810  | 13179  | 498            | 2350 | 4960  | 177               | 655 | 3005  | 7965  |
| 3       | --                  | 6250* | 8584  | 13472  | -              | 7360 | 4525  | -                 | 225 | 7585  | 12110 |

Calculations based on horizontal beds. \* Average of  $B_a$  and  $B_b$ . #Questionable - see text.

Figure 8. Idealized Structural Section from Refraction Survey (see Fig. 4)

### Reflection Data

The continuous reflection profile records were examined and all evidences of sub-bottom structure noted. The line dip of each structure,  $\phi_1$ , i. e., the dip component along the profile, was obtained by measuring the angle of dip as actually recorded on the records,  $\phi_r$  and correcting it for vertical exaggeration to obtain  $\phi_x$ , the apparent line dip, by the relation

$$\tan \phi_x = \tan \phi_r / E \quad (5)$$

The vertical exaggeration (E) for these records was computed from the relation

$$E = 3420 S/V \quad (6)$$

which applies to a record where 36 inches on the vertical axis represents one second of acoustic travel time and 64 inches on the horizontal axis represents one hour of survey time. V is the acoustic velocity in feet per second within the medium comprising the structure and was obtained from results of the refraction studies. S is the actual speed of the survey ship in knots. To minimize the effect of navigation errors, the ship's speed was calculated using the distances between navigation fixes at the ends of each survey leg and

the time taken to survey over that distance.

Because the distance to the reflecting layer is not the vertical distance but the distance along a line which is inclined to the vertical by the angle of line dip ( $\phi_1$ ), the line dip was computed by the relation

$$\phi_1 = \sin^{-1}(\tan \phi_x). \quad (7)$$

The line dips were plotted and true dips of the beds were computed where possible using the graphical method described by Billings (1, p. 443). The results are shown in Figure 9.

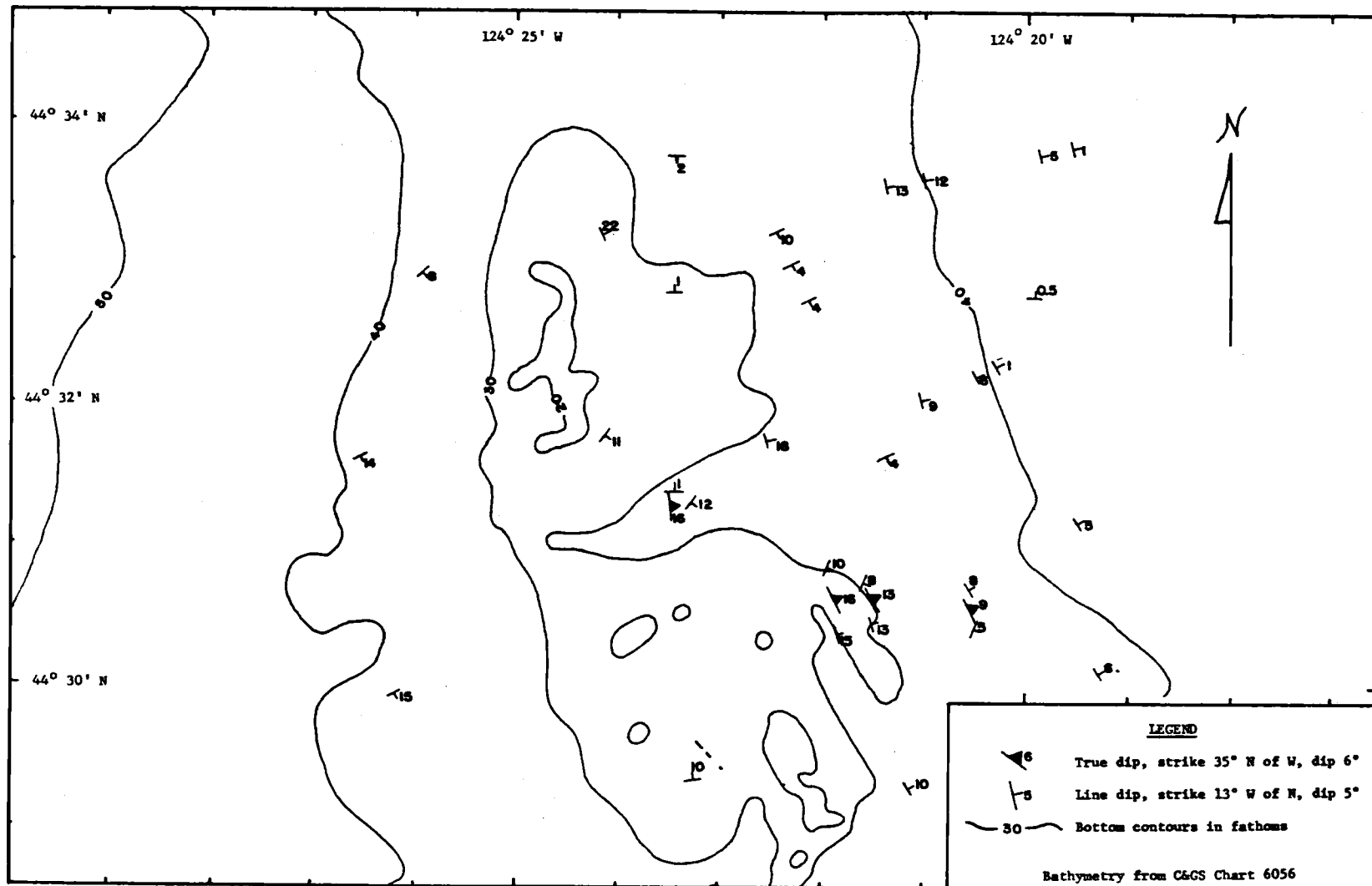


Figure 9. Strikes and dips of structure determined from reflection survey

## DISCUSSION OF RESULTS

In this chapter the results of the refraction survey have been combined with the reflection and bathymetric information and the results of other investigators.

### Surface Morphology

The surface of Stonewall Bank can be divided into three morphological zones as shown in Figure 9. The western boundary of the unconsolidated Quaternary sediments which compose the smooth sea floor east of the Bank lies along the 40 fathom curve. Westward from this boundary, angular dip slope surfaces gradually emerge from beneath the sediments to form the eastern slopes of the Bank. Toward the top of the Bank the surface becomes rough and uneven. This rough surface, characteristic of the top and steeper western slope, extends westward to the 30 fathom curve west of the Bank. This rough surface may be caused by the increased angle between the slope of the sea floor and the emerging bedding planes, especially on the western slope. The structure becomes completely buried beneath the sediments at the 40 fathom curve west of the Bank.

The floor of the east-trending submarine valley which conspicuously divides the Bank in two was flat wherever it was crossed by the survey. One other similar, but much smaller, flat floored

valley was found on the western slope of the Bank a little southwest of the head of the larger valley, but is not shown on Figure 9.

#### Layer A - Unconsolidated Quaternary Sediments

The extent of unconsolidated Quaternary sediments near Stone-wall Bank has been defined by the results of the reflection work augmented by the bathymetric and refraction studies. The data from refraction profiles one and two indicate a layer immediately below the sea floor with a characteristic velocity of approximately 5450 feet per second. The receiving ends of these profiles, shown by solid circles in Figure 4, are in the sediment covered area. Data from profile three do not show any sediments because only a short portion of the receiving end of the profile lies in the sediment covered area. Based on refraction data the calculated thickness of the sediments increases from 250 feet to 500 feet northerly along section A-A', Figure 4. However, at the southern end of the section the reflection data show internal structure less than 50 feet below the sea floor which have an eastward dip component of six degrees. This structure is characteristic of the dips associated with the underlying layer B, and its presence therefore may indicate that the sediment thickness is less than 50 feet rather than 250 feet as calculated from the refraction data assuming flat beds.



### Layer B - Pliocene Siltstones

Maloney and Byrne (2) state that all samples they have collected from Stonewall Bank are varieties of siltstones. These siltstones, with only a few exceptions, dip eastward, increasing from about five or six degrees on the eastern edge where they emerge from beneath the sediments to 16 or more degrees at the top of the Bank where the rougher surface tends to obscure records of internal structure. The few apparent dips which were observed on the western slope do not conflict with the structure observed on the eastern slope but indicate that the dips may continue to increase westward.

Layer B has been defined by combining refraction layers  $B_a$  and  $B_b$ . Arrivals from  $B_a$  are found on all profiles with a characteristic velocity of about 6200 feet per second. Arrivals from  $B_b$ , with a characteristic velocity of 6500 feet per second are found only on profiles one and three and cease abruptly where the profiles cross the Bank in the vicinity of the submarine valley. The travel time curves from  $B_a$  on profiles one and three also have minor discontinuities near the submarine valley. The results of the reflection survey did not reveal the cause of the travel time discontinuities even though the top of  $B_b$ , at a calculated depth of 400 to 700 feet, should be detectable under optimum conditions. Although the proximity of the submarine valley to the position of the travel time

discontinuities strongly suggests a structural relationship, this may be entirely fortuitous.

The thickness of B increases from 2400 feet on the north to 7400 feet on the south along A-A', Figure 4. If the average dip of the structure within B is 12 degrees then approximately 5000 feet of section must be exposed between the 40 fathom curves on either side of the Bank, and consequently the base of B may be beneath the sediments just west of the Bank. Maloney has indicated (personal communication) that samples across the southern part of the Bank within the 40 fathom curve have been identified as Pliocene but that one Miocene sample was obtained at 44-37.2N, 124-26.4W on the 50 fathom curve at the north end of the Bank. Layer B is therefore considered to be Pliocene and if the base of B is exposed west of the Bank and the structure can be extrapolated northward, then the underlying layer C may well be Miocene.

#### Layer C

Layer C has a characteristic velocity of about 8200 feet per second based on an average of the data from profiles two and three. The apparent velocity derived from profile one, 9500 feet per second, was obtained from four data points spread over less than half the horizontal distance occupied by the six data points on profile three and hence warranted less confidence. Although the receiving position

for profiles one and three were essentially identical, the calculated depths to the top of C differed by about 2000 feet. Because the 9500 feet per second apparent velocity from profile one was suspect, an 8000 feet per second line was fitted to the data of profile one and the depth recalculated. The depths agreed within about 300 feet. A value of 8200 feet per second is felt to be the best estimate for the characteristic velocity of layer C obtainable from the present data. The calculated thickness of C decreases from 5000 feet at the north to about 4500 feet at the south end of line A-A' (see Figure 8). The top of the layer has a southerly dip component of about six degrees based on depth calculations from profiles one and two assuming horizontal beds. Assuming profiles one and two are reversed, results in a calculated southerly dip component of six degrees for the top of the layer and a "true" velocity of 8560 feet per second. As mentioned in the preceding section layer C is probably Miocene.

#### Layer D

Arrivals from the top of D were not easily correlated. The amount of energy received varied unsystematically from shot to shot and plotted travel times were scattered. A characteristic velocity for D of 13,300 feet per second was derived by averaging the apparent velocities from profiles two and three. The possibly anomalous apparent velocity of 11,630 from profile one was based

on two arrivals over a short interval and hence did not justify great confidence. Based on depth calculations from profiles two and three, the top of D has a southerly dip component of about six degrees. Assuming profiles one and two are reversed and using the uncertain velocity of 11,630 feet per second from profile one, results in a calculated dip of seven and one-half degrees to the north for the top of D. The often irregular or absent arrivals from the top of D probably result from a combination of insufficient source energy and an uneven and possibly complex surface. Although the characteristic velocity of 13,300 feet per second does not rule out the possibility of D being basement rock, it is not considered probable unless supported by additional evidence.

## CONCLUSIONS

The results of this study are a north-south structural section, Figure 8, along the eastern side of the Stonewall Bank and a description of the submarine morphology and internal structure of the Bank. The evidence indicates that the Bank is formed by eastward dipping Pliocene siltstones emerging westward from beneath unconsolidated Quaternary sediments. The dip of the siltstones increases across the Bank from five or six degrees on the east to 16 or more degrees on the west. There is little evidence of significant structural complexity in the studied area. The refraction data indicates that the Pliocene siltstones thicken southward by 5000 feet along the A-A', accounting for most of the increase in thickness of the measured section. The underlying layer C, tentatively thought to be Miocene, may crop out west of the Bank beneath the unconsolidated sediments. This formation, about 5000 feet thick, has a southerly dip component of six to seven degrees. The depth to the base of layer C on the north, 8000 feet, agrees well with that computed independently by Whitcomb (5, p. 28) from gravity data for the base of a layer having a density of 2.15 grams per cubic centimeter. His calculated basement depths of about 20,000 feet would indicate that the top of D, at 8000 feet, is not the top of basement. The interface at the top of D has a southerly dip component of about six degrees and lies about 12,000 feet below the southern part of the Bank.

## BIBLIOGRAPHY

1. Billings, Marland P. Structural geology. 2d ed. New York, Prentice-Hall, 1954. 514 p.
- 1a. Byrne, John V. Geomorphology of the continental terrace off the central coast of Oregon. *The Ore Bin* 24: 65-74. 1962.
2. Maloney, Neil J. and John V. Byrne. Sedimentary rocks from the continental shelf and slope off the central coast of Oregon. *The Ore Bin* 26: 77-83. 1964.
3. Officer, Charles B. Introduction to the theory of sound transmission. New York, McGraw Hill, 1958. 284 p.
4. Officer, Charles B. et al. Geophysical investigations in the eastern Caribbean: Summary of 1955 and 1956 cruises. In: *Physics and chemistry of the earth*, ed. by L. H. Ahrens et al., Vol. 3. London, Pergamon Press, 1959. p. 17.
5. Whitcomb, James H. Marine geophysical studies offshore--Newport, Oregon. Master's thesis. Corvallis, Oregon State University, 1964. 51 numb. leaves.